

Decisive role of fluctuations in the resource dependency networks

Saumitra Kulkarni and Snehal M. Shekatkar*

*Department of Scientific Computing, Modeling and Simulation,
Savitribai Phule Pune University, Pune 411007, India*

Individual components of many real-world complex networks produce and exchange resources among themselves. However, because the resource production in such networks is almost always stochastic, fluctuations in the production are unavoidable. In this paper, we study the effect of fluctuations on the resource dependencies in complex networks. To this end, we consider a modification of a threshold model of resource dependencies in networks that was recently proposed, where each vertex can either be in a *fit* or a *degraded* state. We study how the “network fitness” is affected as the fluctuation size is varied. We show that, the relative value of the average production with respect to the threshold, decides whether the fluctuations are beneficial or detrimental to the network fitness. We further show that the networks with a homogeneous degree distribution, such as the Erdős-Rényi network, perform better in terms of fitness and also produce lower wastage than the Scale-Free network. Our work shows that, in the study of resource dependencies in networks, the role of the fluctuations is as decisive as the average production.

I. INTRODUCTION

Complex networks have emerged as a unifying framework to study the real-world complex systems that are made up of a large number of individual elements or units [1, 2]. Components of most real-world complex system require adequate amount of one or more resources for proper functioning and for survival. Some common examples include water and food required by humans, electricity required by computers and routers, and raw material required by manufacturing firms. Usually the components need some threshold amount of a resource so that if the amount is less than the threshold of a component, its performance degrades or the component may die altogether. An important point of consideration is that a given component may not be capable of producing a required resource or may not produce it as much as it is required, and hence needs to procure some amount from other components of the system. For example, not every human being produces food material but can get it from other humans who do produce it. Similarly, most manufacturing firms do not produce their own electricity, and hence must buy it from entities like electricity boards. These links between components of a bigger system can be viewed as a complex network in which nodes produce various resources and share the surplus amounts to others which need those [3, 4]. Trade networks, in which resources are exchanged for money or other resources is a classic example of such network [5–10].

In the manufacturing industry, supply chains are of utmost importance. Fundamentally, supply chains are networks of firms or manufacturing entities in which raw materials are procured and converted into ancillary or final products. There have been many attempts of modelling the dynamics of supply-chains [11, 12]. The goal of such modelling efforts is to try to maximize their in-

dividual profit and livelihood [13–17].

A related network type in which some resource flows from one vertex to another is distribution networks. Some examples of distribution networks are power-grids [18, 19], networks of gas pipelines [20], river networks [21–24], cardiovascular and respiratory networks [25, 26], and plant vascular and root systems [27–29].

All these networks mentioned above fall under a more general category of networks called the *resource dependency networks* in which the vertices depend on each other for various resources. In this work, we aim to advance the work related to such networks that have recently been studied from a perspective of complex networks [3, 4]. We particularly want to find out how the fluctuations in the production can affect the quality of the state of the network as quantified by *Network Fitness* in our work. A major difference between these previous studies and the present one is that when a vertex does not have a threshold amount, instead of dying, it just goes into a degraded state. This is true in most real-world scenarios.

The rest of the paper is organized as follows. In Sec.II we present a variation of the model of resource dependency in [3]. In this section, apart from the model description, we also describe the way we are using different probability distributions to generate resource at each vertex as well as the process of generating substrate networks to carry out simulations. In Sec.III, we describe the simulation results obtained by varying the fluctuation size in the resource generation. After that in Sec.IV we describe how the fluctuations affect the amount of resource wastage in a network, and we conclude in Sec.V.

II. SURPLUS DISTRIBUTION MODEL

The model that we use here is a variation of the model of resource dependencies proposed in [3]. Consider a network with n vertices and m edges. Each vertex i in the network stochastically produces amount $X_i(t)$ at each

*snehal@inferred.in

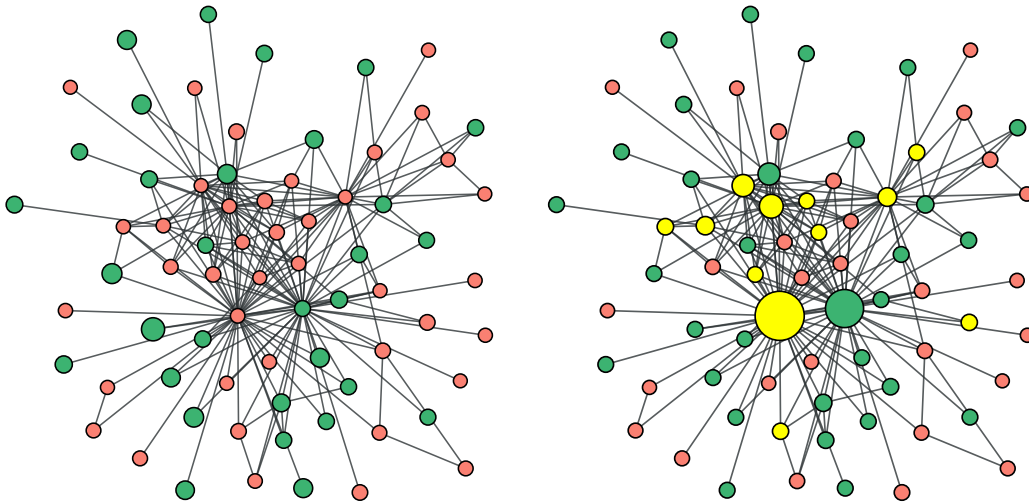


FIG. 1: Graphical representation of the *Surplus Distribution Model*. (Left) Each vertex i produces resource amount X_i . The vertices for which $X \geq R$ are in the *fit state* (shown in green). The vertices with $X < R$ are shown in red. (Right) Every vertex with $X > R$ shares its surplus $X - R$ equally with its neighbours. Each vertex j which had $X_j < R$ but now has received enough amount from its neighbours such that the total resource amount on it $X_j^{\text{tot}} > R$, also transitions into the *fit state* (shown in yellow). The remaining vertices go into a *degraded state* (shown in red). In this picture, the sizes of vertices approximately indicate the amount present on them.

discrete time $t = 0, 1, 2, \dots$. This amount X_i is a random variable with some probability distribution $p(x, \beta_i)$ where β_i is the collection of parameters of the distribution. Also, each vertex i requires a threshold amount R_i of resource to be in a *fit state*. If $X_i(t) > R_i$, vertex i has *surplus* $X_i(t) - R_i$, which it distributes equally among all its neighbours. If $X_i(t) < R_i$, there is no surplus and consequently no sharing happens. Thus the total amount on each vertex i at time t can be written as:

$$X_i^{\text{tot}}(t) = \begin{cases} X_i(t) + \sum_{j=1}^n A_{ij} \frac{S_j(t)}{k_j} & \text{if } X_i(t) < R_i \\ R_i + \sum_{j=1}^n A_{ij} \frac{S_j(t)}{k_j} & \text{Otherwise} \end{cases} \quad (1)$$

Here A_{ij} denotes the $(i, j)^{\text{th}}$ element of the adjacency matrix of the network, k_j is the degree of vertex j , and the $S_j(t)$ is the amount of *surplus* on vertex j at time t :

$$S_j(t) = \max(X_j - R_j, 0) \quad (2)$$

An important aspect of the model is that the resource is assumed to have a lifetime of only 1 unit of time. This assumption is valid for many perishable resources in the real-world which include agricultural goods like vegetables, fruits etc. and dairy products like milk. In line with this, we assume that if $X_i^{\text{tot}}(t) < R_i$, the vertex i completely consumes it at time t . But if $X_i^{\text{tot}}(t) > R_i$, the vertex only consumes the amount R_i , and the remaining amount $X_i^{\text{tot}}(t) - R_i$ is discarded at

time t , and none is left for time $t + 1$. As stated above, if $X_i^{\text{tot}}(t) \geq R_i$, we say that the vertex i is in a *fit state*, otherwise it is in a *degraded state* at time t . Fig. 1 shows a graphical representation of this model.

Let us denote the probability distribution of X_i^{tot} by $Q_i(x)$. Then the probability that the vertex i is in a fit state is given by:

$$p_i = \int_{R_i}^{\infty} Q_i(x) dx \quad (3)$$

Note that, in general, the distribution $Q_i(x)$ for the vertex i , apart from depending upon $p(x; \beta_i)$, would also depend on the topological characteristics of the vertex like its degree, centrality, clustering coefficient etc. Thus, even when all the parameters β_i of the producing distribution are same, the distribution $Q(x)$ and hence the probability p of being in a fit state, are in general different for different vertices. Moreover, since the network state at time $t+1$ is completely independent of the state at time t , the distribution $Q_i(x)$ and p_i are time-independent. This also means that the parameter t is redundant in our model. But keeping this parameter makes the model flexible so that it might be possible to extend it to Markovian dynamics or even to non-Markovian dynamics.

A quantity of interest to us is the fraction of vertices in the network which are in a fit state at any given time, which in the limit of an infinite sized network is given by:

$$F = \lim_{n \rightarrow \infty} \frac{1}{n} \sum_{i=1}^n p_i \quad (4)$$

We call F the *Network fitness*, and in the rest of the paper, we investigate how it is affected by the network topology and the fluctuations in the resource production on vertices.

Since the quantity F in Eq(4) is defined for an infinite sized network, we must find a way to estimate its value computationally using an ensemble of only finite sized networks. To do that, let us consider the following estimator for F :

$$\widehat{F}(t) = \frac{1}{n} \sum_{i=1}^n H(X_i(t) - R_i) \quad (5)$$

where $H(x)$ denotes the Heaviside step function defined to be 1 for $x \geq 0$ and 0 otherwise. Because the networks we use to simulate the model contain only a finite number n of vertices, this quantity would fluctuate with time. However, as n increases, the fluctuations in \widehat{F} would reduce in size. Because $Q_i(x)$ is time-independent, we can modify the estimator given above to include the time average as follows:

$$\widehat{F} = \lim_{T \rightarrow \infty} \frac{1}{T} \sum_{t=0}^T \left(\frac{1}{n} \sum_{i=1}^n H(X_i(t) - R_i) \right) \quad (6)$$

Since now we have average over more replications, this estimator estimates F more precisely. A central question that we investigate in this paper is whether for a given network topology, we can maximize F by changing the size of fluctuations in the produced amount.

A. Choice of probability distributions

In this paper, we are interested in studying the effect of fluctuations, and for this, we must choose those distributions in which the fluctuation size can be varied keeping the mean fixed. Henceforth we will use the term *resource generator* to refer to a probability distribution that is used to stochastically generate resource at each vertex. In the resource dependency model proposed in [3], the resource generator was the *exponential* distribution $p(x) = \text{Exp}(x, \beta)$. However, for the exponential distribution, the mean and the standard deviation are equal, and hence it is not possible to vary the fluctuation size independent of mean. Thus, it was not possible there to separate the effects of the average production and the fluctuation size. For this reason, here we use Gaussian and Pareto distributions as resource generators. These two serve as prototypes of the classes of peaked and heavy-tailed distributions respectively.

The usual Gaussian distribution has the whole real line as its support. However, the resource amount cannot be negative. Hence we use the *truncated* Gaussian distribution which is obtained by removing the negative tail of the usual Gaussian distribution. The probability density of this distribution is given by:

$$p(x; \mu, \sigma) = \frac{1}{\psi(\mu, \sigma)} \exp\left(-\frac{(x - \mu)^2}{2\sigma^2}\right) \quad (7)$$

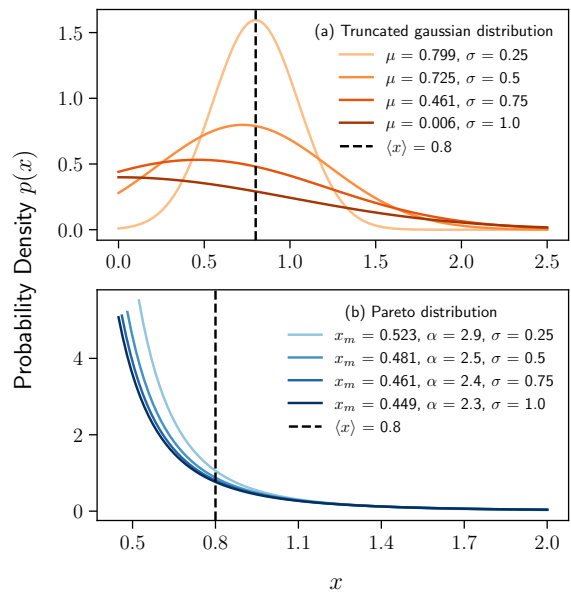


FIG. 2: Probability density curves for the truncated Gaussian and the Pareto distributions for different sizes of fluctuation σ with the mean of the distribution $\langle x \rangle$ fixed at 0.8. For the truncated Gaussian, the parameter μ decreases as σ increases. For the Pareto distribution, both x_m and α decrease as σ increases. Vertical dashed line marks the mean $\langle x \rangle$ of the distribution in both the subplots.

where,

$$\psi(\mu, \sigma) = \int_{x=0}^{\infty} \exp\left(-\frac{(x - \mu)^2}{2\sigma^2}\right) dx \quad (8)$$

In the case of usual Gaussian distribution $\mathcal{N}(\mu, \sigma^2)$, the mean of the distribution $\langle x \rangle$ is equal to μ , and hence is independent of σ . However, for the truncated Gaussian distribution, the mean is a function of both μ and σ because truncation makes the distribution asymmetrical. In fact, the mean is given by:

$$\langle x \rangle = \frac{1}{\psi(\mu, \sigma)} \int_{x=0}^{\infty} x \exp\left(-\frac{(x - \mu)^2}{2\sigma^2}\right) dx \quad (9)$$

To vary the fluctuation size, we can vary σ . However, if we do that keeping μ at a fixed value, the mean $\langle x \rangle$ also changes: increasing σ leads to a flatter distribution resulting in the higher value of $\langle x \rangle$. For this reason, while increasing σ , we simultaneously decrease μ so that the mean remains fixed. This is an important consideration because we specifically want to study how changing the fluctuation size affects the network fitness for the same value of the average production. Since the integral in Eq(9) cannot be computed analytically, we numerically integrate it for a given value of σ by systematically varying μ so as to find the value for which the R.H.S. of Eq(9) is equal to a given value of $\langle x \rangle$ within a numerical error.

For the Pareto distribution, we have to use a similar strategy. The Pareto distribution is a continuous probability distribution with support $[x_m, \infty)$ where the parameter $x_m > 0$. The density of the Pareto distribution is:

$$p(x; x_m, \alpha) = \frac{\alpha x_m^\alpha}{x^{\alpha+1}} \quad (10)$$

where α is the shape parameter which decides how steep the distribution is. For this distribution, the mean exists only for $\alpha > 1$, and is the function of both x_m and α :

$$\langle x \rangle = \frac{\alpha x_m}{\alpha - 1} \quad (11)$$

Also, for the Pareto distribution the standard deviation exists only for $\alpha > 2$, and is given by:

$$\sigma = \sqrt{\frac{\alpha x_m}{(\alpha - 1)^2(\alpha - 2)}} \quad (12)$$

Eliminating x_m from Eq(11) and Eq(12), we get:

$$\alpha = 1 + \sqrt{1 + \frac{\langle x \rangle^2}{\sigma^2}} \quad (13)$$

Thus, to vary the fluctuations, we vary σ in the range $(0, 1)$ for a given $\langle x \rangle$. For each value of σ , we get a unique value of α from this equation. Then the Eq(11) gives us x_m corresponding to these σ and $\langle x \rangle$ which can then be used to simulate the model. It is worth noting that as σ increases, both x_m and α decrease. This fact will be useful to us in the discussion ahead.

Thus for both truncated-Gaussian and Pareto generators, we use $\langle x \rangle$ as a parameter of the model which can be fixed to a suitable value, and then we vary the fluctuation size by changing σ to see how the network fitness is affected. We present the simulation results in Sec.III.

B. Generation of substrate networks

Apart from the parameters of the producing distribution $p(x; \beta_i)$, the Network Fitness F is also affected by the network topology. In this paper, we restrict ourselves to studying only the degree distribution of the network. In particular, we want to see how the fluctuations in the generation of resources affect the network fitness for two typical classes of degree distributions: peaked and heavy-tailed. As archetypal examples of these two classes, we choose Poisson and Power-law degree distributions. The configuration model of networks is a random graph model with a given degree sequence. However, in the limit of large network size ($n \rightarrow \infty$), this model can be thought of as a random graph model with a given degree distribution if a degree sequence is drawn from the specified distribution [30]. As mentioned above, in this paper we are only interested in studying the effect of degree-distribution on

the network fitness, and hence we use the configuration model with Poisson and Power-law degree distributions to generate the substrate networks. The corresponding networks are also known as the Erdős-Rényi network and the Scale-free network respectively. Henceforth, in this paper we refer to these two networks as ER and SF networks respectively. The only problem with the use of the configuration model is that it also allows multi-edges and self-loops. In our simulations, we remove all self-loops and we collapse all the multi-edges to single weighted edges with weights given by corresponding multiplicities. We then make the fraction of surplus shared along each edge proportional to its weight.

It is important to make sure while comparing results for ER and SF networks that they have the same average degree. If k_{\min} denotes the minimum degree value in a SF network, its normalized power-law degree distribution has the form:

$$p_k = \frac{k^{-\alpha}}{\zeta(\alpha, k_{\min})} \quad \text{for } k \geq k_{\min} \quad (14)$$

while $p_k = 0$ for $k < k_{\min}$. Here α is the scaling index of the power law and $\zeta(\alpha, k_{\min})$ is the Hurwitz zeta function. If we draw degree values from this distribution, the value of the average degree is given by:

$$\langle k \rangle_{SF} = \sum_{k=k_{\min}}^{\infty} k p_k = \sum_{k=k_{\min}}^{\infty} \frac{k^{1-\alpha}}{\zeta(\alpha, k_{\min})} \quad (15)$$

In this paper, we choose $k_{\min} = 2$ and $\alpha = 2.2$ which gives $\langle k \rangle_{SF} \approx 9.36$. To make the right comparison with the SF network, we sample the degree values for the ER network from the Poisson distribution:

$$p_k = e^{-\langle k \rangle_{SF}} \frac{\langle k \rangle_{SF}^k}{k!} \quad (16)$$

This way, both types of networks theoretically have the same average degree.

III. EFFECT OF FLUCTUATIONS

In this paper, we assume that the average production $\langle x \rangle$ is same for all the vertices. We also assume that the thresholds R_i have the same value $R = 1$ for all the vertices. Unless mentioned otherwise, all the numerical simulation results presented in this paper are obtained by averaging over 100 realizations of networks each of size $n = 10^4$. Also, for each realization, the model is simulated for $t = 1000$ time steps. All the codes used in this paper are freely available as a part of the Python library *dependency-networks* [31].

A. Effect of generators

As we describe in this section, the type of generator (Gaussian vs Pareto) has a significant impact on the network fitness. To systematically study it, we consider the

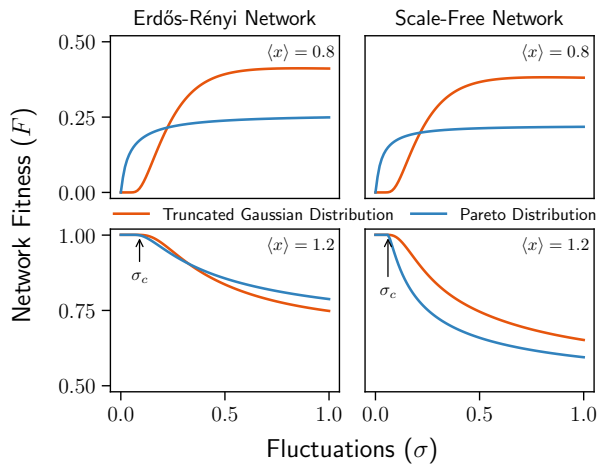


FIG. 3: Variation of network fitness with fluctuation size for different combinations of network topologies, resource generators and average productions. *Left* and *Right* columns correspond to ER and SF topologies, while the *Top* and *Bottom* rows correspond to $\langle x \rangle < R$ and $\langle x \rangle > R$ respectively. The σ_c denotes the critical σ that separates completely fit and partially fit states for the Pareto generator. See text for a detailed discussion.

cases $\langle x \rangle < R$ and $\langle x \rangle > R$ separately. The results that we present below are obtained by varying fluctuation size σ for various combinations of the generator and network topology when $\langle x \rangle < R$ and $\langle x \rangle > R$. Let us first consider the case where the average resource $\langle x \rangle$ production on each vertex is less than the threshold. Top panels in Fig. 3 shows the variation of F as we vary σ for both ER and SF networks and for both Gaussian and Pareto generators when $\langle x \rangle = 0.8$. We see that as we increase the size of fluctuations starting from zero, the network fitness also starts increasing, and saturates to a value less than 1 for both truncated-Gaussian and Pareto generators. From these plots, it is also clear that whether the Gaussian generator performs better or worse than the Pareto generator depends upon the value of σ . However, it is clear that when $\langle x \rangle < R$, the fluctuations improve the performance of the network. Moreover, we also see that beyond a point, increasing the fluctuation size has no effect on the fitness.

Interestingly, when $\langle x \rangle > R$, increasing the fluctuation size σ worsens the fitness F independent of the generator and the network topology (bottom panels of Fig. 3). Also, as the figure shows, in this case, for the Pareto generator there exists a value $\sigma = \sigma_c$ below which the network remains in a completely fit state ($F = 1$). For $\sigma > \sigma_c$, the network transitions into a state of partial fitness. We discuss the reasoning behind the existence of this critical σ_c in subsection III B. In both these cases ($\langle x \rangle < R$ and $\langle x \rangle > R$), Fig. 3 might give an impression that for the Gaussian generator also there exists a critical σ value below which the network remains in a completely unfit state ($F = 0$ for $\langle x \rangle < R$) or a completely fit state

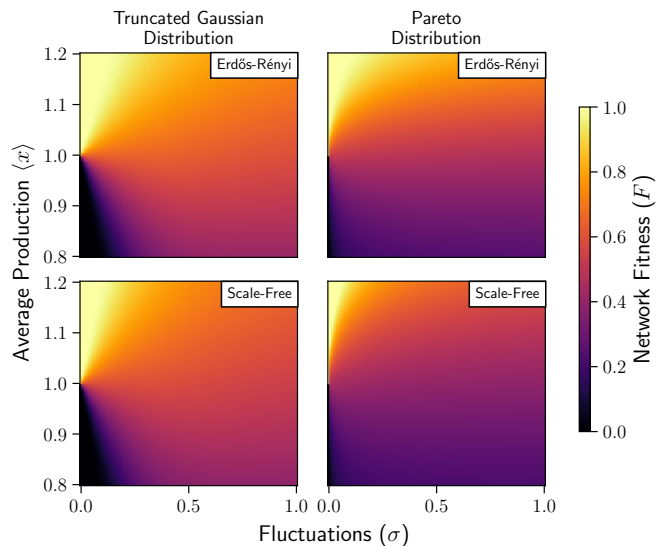


FIG. 4: Heatmaps showing the variation of network fitness in the $\langle x \rangle$ - σ plane for different combinations of network topologies and resource generators. *Left* and *Right* columns correspond to the two different generators, while the *Top* and *Bottom* rows correspond to ER and SF topologies respectively. The results are obtained by averaging over 1000 time steps and 100 realizations of networks of size 1000 each.

($F = 1$ for $\langle x \rangle > R$). However, this is not true as the following argument shows. When $\langle x \rangle < R$, the probability that a vertex produces value greater than the threshold R is:

$$\int_{x=R}^{\infty} p(x; \mu, \sigma) dx = \frac{1}{\psi(\mu, \sigma)} \int_{x=R}^{\infty} \exp\left(-\frac{(x-\mu)^2}{2\sigma^2}\right) dx \quad (17)$$

Since the exponential function in this integral is neither exactly zero nor is negative for any $x \geq R$, this integral cannot be exactly zero. When $\langle x \rangle < R$ and σ is small, this integral turns out to be very close to zero, and numerical solutions tend to produce zero values. In other words, although practically we might see $F = 0$ for $\langle x \rangle < R$ for small values of σ , theoretically that is not true, and hence no critical σ exists for the Gaussian generator. A similar argument would show that $F = 1$ is not possible when $\langle x \rangle > R$ for any value of σ because there is always some portion of the density function below R , and hence a critical σ_c cannot exist.

B. Effect of network topology

In this section, we discuss the effect of network topology on the fitness. In Fig. 5, we compare $F(\sigma)$ for both ER and SF networks where different panels correspond to different combinations of $\langle x \rangle$ and generator. For a given combination, changing the structure of the network changes the quantitative behavior of $F(\sigma)$, but not the qualitative behavior. We also see that irrespective of the

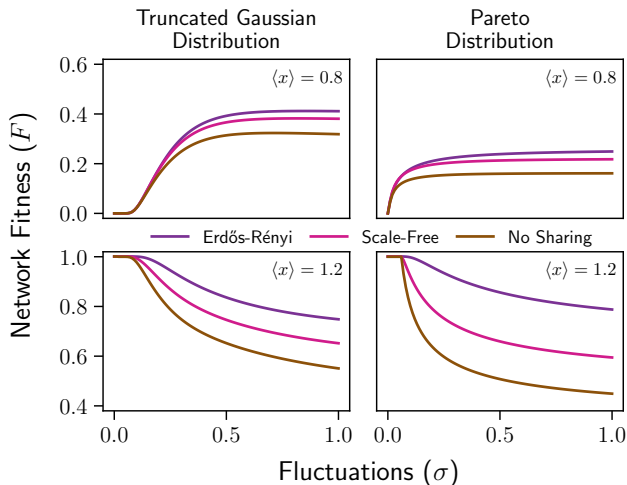


FIG. 5: Comparison of network fitness curves of ER and SF topologies for various combinations of average productions and resource generators. The brown curve in each subplot shows the lower bound F_L obtained analytically by considering a network in which vertices are not allowed to share their surplus amounts. *Left* and *Right* columns correspond to the two different generators, while the *Top* and *Bottom* rows correspond to $\langle x \rangle < R$ and $\langle x \rangle > R$ respectively.

combination used, the ER network performs better than the SF network. We note here that a similar conclusion has been reached in earlier works too [3, 4]. To separately understand the effect of network topology on the fitness for the two generators, let us first consider a case in which the vertices are not allowed to share their surplus with other vertices. The fitness F_L corresponding to this *No-sharing* situation is the lower bound for fitness for any network where sharing is allowed. It is easy to see that F_L is just the probability that a vertex produces amount greater than the threshold R .

The value of F_L for the Gaussian generator is given by:

$$F_L^{gauss} = \frac{1}{\psi(\mu, \sigma)} \int_{x=R}^{\infty} \exp\left(-\frac{(x-\mu)^2}{2\sigma^2}\right) dx \quad (18)$$

To compute F_L as a function of σ , as described in Sec.IIA, we compute the value of the parameter μ for a given σ such that the average production $\langle x \rangle$ remains at a fixed value. We then perform the integral in this equation numerically using this obtained value of μ for a given σ .

We can compute F_L^{parato} in as we describe now. Rearranging Eq(11) for x_m , we get:

$$x_m = \left(1 - \frac{1}{\alpha}\right) \langle x \rangle \quad (19)$$

When $\langle x \rangle < R$, this equation implies $x_m < R$ for all

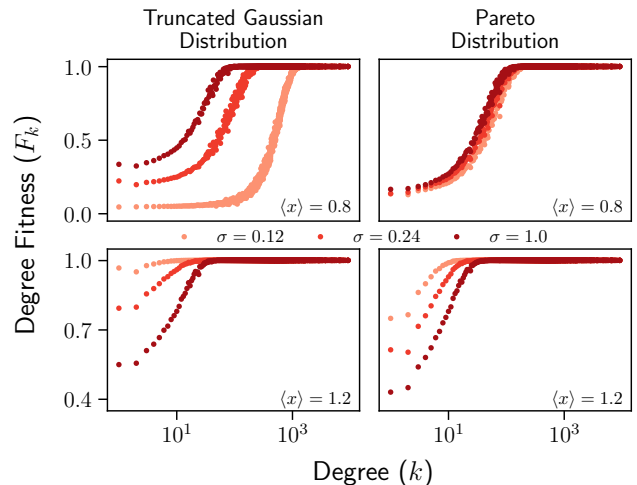


FIG. 6: Scatterplots of *degree fitness* (average fitness of vertices of a given degree) and degree for three different fluctuation sizes for the SF network. *Left* and *Right* columns correspond to the two different generators, while the *Top* and *Bottom* rows correspond to $\langle x \rangle < R$ and $\langle x \rangle > R$ respectively. Although the quantitative behavior of the plots is different for different combinations of generators and average productions, it can be seen that the fitness tends to increase with degree.

values of α . Hence in this case:

$$F_L^{parato} = \int_R^{\infty} \frac{\alpha x_m^\alpha}{x^{\alpha+1}} dx = \left(\frac{x_m}{R}\right)^\alpha = \left(1 - \frac{1}{\alpha}\right)^\alpha \left(\frac{\langle x \rangle}{R}\right)^\alpha \quad (20)$$

For $\langle x \rangle < R$, the ratio $\langle x \rangle / R < 1$, which means that in this case F_L would increase with increase in σ , and as $\sigma \rightarrow \infty$, $\alpha \rightarrow 2$, which implies that asymptotically $F_L^{parato} \rightarrow \langle x \rangle^2 / 4R^2$. From Eq(19), when $\langle x \rangle > R$, whether $x_m < R$ or $x_m > R$ depends on the value of α . Therefore there exists a transition value α_c such that for $\alpha < \alpha_c \Rightarrow x_m < R$ while $\alpha > \alpha_c \Rightarrow x_m > R$. For the transition value α_c , $x_m = R$ and Eq(19) gives:

$$R = \left(1 - \frac{1}{\alpha_c}\right) \langle x \rangle \Rightarrow \alpha_c = \frac{\langle x \rangle}{\langle x \rangle - R} \quad (21)$$

Using this α_c in Eq(13), we get the corresponding transition value σ_c :

$$\alpha_c = \frac{\langle x \rangle}{\langle x \rangle - R} = 1 + \sqrt{1 + \frac{\langle x \rangle^2}{\sigma_c^2}} \quad (22)$$

which gives:

$$\sigma_c = \frac{\langle x \rangle (\langle x \rangle - R)^2}{2R - \langle x \rangle} \quad (23)$$

For $\sigma < \sigma_c \Rightarrow x_m > R$, and hence the lower bound

F_L^{pareto} is given by:

$$F_L^{pareto} = \int_{x_m}^{\infty} p(x; x_m, \alpha) dx = 1 \quad (24)$$

Whereas, for $\sigma > \sigma_c$, F_L^{pareto} is given by Eq(20). Thus, we see that unlike the case $\langle x \rangle < R$, here we have two distinct regions in which qualitatively different behaviors are seen. In the region $\sigma < \sigma_c$, the network is in a completely fit state whereas as soon as σ crosses σ_c , it goes into a partially fit state.

The brown curve in each subplot in Fig. 5 shows the variation of F_L with σ . The plots in the figure also show that the actual shape of $F(\sigma)$ is not qualitatively very different from $F_L(\sigma)$. This means, the only effect of sharing is to scale the curves up. Furthermore, it is also clear that sharing smoothens the transition at σ_c that is observed for the Pareto generator.

The fitness of a network is the average of fitness values of all the vertices in the network. However, the vertices are not equivalent in terms of fitness because they are not equivalent in terms of topology. In fact, it is clear from Eq(1) that a vertex receives amount approximately proportional to its degree. Because of this, the high-degree vertices tend to be fit more often than the low-degree vertices. To verify this, we define the quantity *Degree fitness* F_k which is just the average fitness of a vertex with degree k . In Fig. 6, we show scatterplots of F_k and k for various combinations of $\langle x \rangle$, σ , generator for the SF network. As is evident from these plots, independent of the choice of these parameters, fitness is a rapidly increasing function of the degree, and for relatively small values of degree, the degree fitness reaches its maximum value 1.

IV. WASTAGE

After the surplus amounts are distributed to the neighbours, if the amount X_i^{tot} on vertex i is greater than its threshold R_i , the vertex goes into a fit state. However, out of X_i^{tot} , only amount R_i is consumed by the vertex and the remaining amount $w_i = (X_i^{\text{tot}} - R_i)$ is wasted. It would be interesting to find out the how the total amount of wastage per unit time per vertex varies in the network. This wastage can be formally written as:

$$w = \lim_{n \rightarrow \infty} \lim_{T \rightarrow \infty} \frac{1}{nT} \sum_{t=1}^T \sum_{i=1}^n w_i(t) H(w_i(t)) \quad (25)$$

Fig. 7 compares the wastage variation with σ for ER and SF networks with different combinations of $\langle x \rangle$ and resource generator. As these plots show, in all the cases the ER network has lower wastage compared to the SF network. This is because the degree distribution of the ER network is more homogeneous and hence the generated resource is distributed more uniformly compared to the SF network. Because of this, the ER network tends

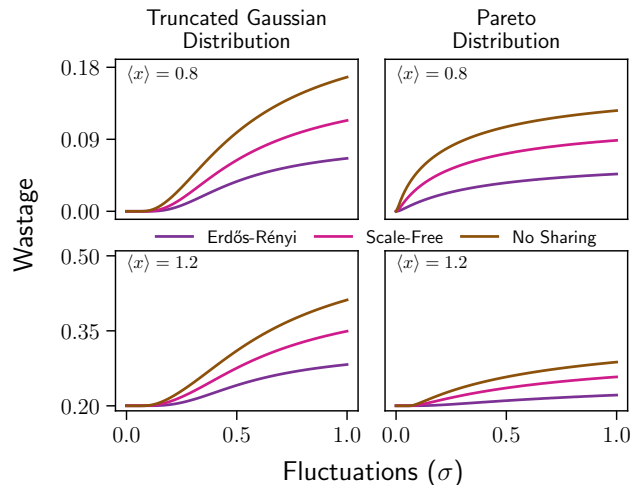


FIG. 7: Comparison of wastage curves for ER and SF topologies for various combinations of average productions and resource generators. *Left* and *Right* columns correspond to the two different generators, while the *Top* and *Bottom* rows correspond to $\langle x \rangle < R$ and $\langle x \rangle > R$ respectively. The brown curve in each subplot shows the analytically obtained wastage when vertices are not allowed to share their surplus. As the plots show, although wastage strongly depends on $\langle x \rangle$ and the generator used, the ER network always leads to lesser wastage than the SF network.

to be more fit than the SF network as we have seen in the previous section.

We can also better understand the actual wastage variation if we look at the wastage amount in the “No-sharing” case. Clearly, if the vertices are not allowed to share their surplus amounts, there would be maximum possible wastage in the network. This provides us with an upper bound W for w . For the truncated Gaussian distribution, this upper bound can be written as:

$$W^{\text{gauss}} = \frac{1}{\psi(\mu, \sigma)} \int_R^{\infty} (x - R) \exp\left(-\frac{(x - \mu)^2}{2\sigma^2}\right) dx \quad (26)$$

Although this integral cannot be computed analytically, as described in the previous section, we can vary σ and simultaneously adjust μ so that $\langle x \rangle$ remains fixed at a chosen value, and look at how the wastage W^{gauss} changes by numerically computing the integral.

We can obtain the upper bound for the Pareto distribution also, but the situation is somewhat more complicated. Here also we would like to see how the wastage varies as σ is varied while keeping $\langle x \rangle$ at a fixed value. But as we have seen in Sec.II A, both α and x_m decrease as σ is increased. There we also saw that as long as $\sigma < \sigma_c$, $x_m > R$ which in turn means that $x > R$, and hence the expected wastage on a single vertex, when

sharing is not allowed, is:

$$W_{(\sigma \leq \sigma_c)}^{pareto} = \int_{x_m}^{\infty} (x - R)p(x)dx = \alpha x_m^\alpha \int_{x_m}^{\infty} \frac{x - R}{x^{\alpha+1}} dx \quad (27)$$

For $\sigma > \sigma_c$, $x_m < R$ and hence the expected wastage in absence of sharing is:

$$W_{(\sigma > \sigma_c)}^{pareto} = \int_R^{\infty} (x - R)p(x)dx = \alpha x_m^\alpha \int_R^{\infty} \frac{x - R}{x^{\alpha+1}} dx \quad (28)$$

Evaluating the integrals in (27) and (28), we get the expected wastage on a single vertex as:

$$W^{pareto} = \begin{cases} \frac{R^{1-\alpha}}{\alpha-1} \langle x \rangle^\alpha \left(1 - \frac{1}{\alpha}\right)^\alpha & \text{if } \sigma \leq \sigma_c \\ \langle x \rangle - R & \text{otherwise} \end{cases} \quad (29)$$

where α is given by Eq(13).

The brown curves in Fig. 7 show the curves for the upper bound W . Similar to the case of network fitness, we see that the qualitative variation of w for ER and SF networks is similar to that of W . The only effect of sharing is to scale the W curve down.

V. CONCLUSION

In this work we studied how fluctuations in the generation of a resource on vertices of the network affects its fitness. Generation of resource in our work is modelled by truncated Gaussian and Pareto distributions. We chose these particular distributions because they are prototypes of peaked and heavy-tailed distributions respectively. While changing the fluctuation size in both these cases we made sure that the average production on a vertex remains fixed, and hence our results are solely driven by fluctuations alone.

We simulated our *surplus distribution model* on ER and SF networks with the same average degree. We found

that, depending upon the average production, fluctuations can either improve the network fitness or deteriorate it. We also verified a similar result of earlier works that resource dependency networks with the ER topology perform better than those with the SF topology. We have analytically obtained the lower bound on the network fitness in all the cases, and explained the sharp transitions observed for Pareto generator. Using this, we also showed how the network topology only scales up the fitness curves. We also showed how the network fitness is linked with the amount of resource wasted in the network. Furthermore we analytically computed the upper bound for the wastage in these cases.

The main insight provided by our work is that fluctuations may be beneficial or detrimental to a resource dependency network. This depends upon whether the average production on each vertex is less than or greater than its threshold. This work can be extended further in a number of directions. In this work, the production capacity of every vertex is assumed to be same. It would be interesting to see how fluctuations affect the network fitness when that is not the case. For example, production capacity can be made a function of vertex degree or of some other centrality measure like eigenvector or betweenness. Similar to heterogeneity in the average production, the case of different fluctuation sizes for different vertices can also be explored. Moreover, in this work we focused only on the degree distribution of a network, but it is possible to study the effect of other structural properties like degree correlations, clustering, and community structure which can potentially affect the network fitness. We plan to explore these directions in future work.

Acknowledgments

SMS acknowledges funding from the DST-INSPIRE Faculty Fellowship (DST/INSPIRE/04/2018/002664) by DST India. SK acknowledges the fellowship received under the same scheme to work on the project. SMS would like to thank Sitabhra Sinha whose comment about fluctuations led SMS to conceive this project.

-
- [1] M. Newman, *Networks* (Oxford university press, 2018).
 - [2] R. Albert and A.-L. Barabási, *Reviews of modern physics* **74**, 47 (2002).
 - [3] M. Ingale and S. M. Shekatkar, *Phys. Rev. E* **102**, 062304 (2020).
 - [4] H. Agrawal, A. Lahorkar, and S. M. Shekatkar, *Europhysics Letters* **139**, 51003 (2022).
 - [5] D. Garlaschelli and M. I. Loffredo, *Phys. Rev. Lett.* **93**, 188701 (2004).
 - [6] M. Di Vece, D. Garlaschelli, and T. Squartini, *Phys. Rev. Research* **4**, 033105 (2022).
 - [7] D. Garlaschelli and M. I. Loffredo, *Phys. Rev. Lett.* **93**, 188701 (2004).
 - [8] T. Squartini, G. Fagiolo, and D. Garlaschelli, *Phys. Rev. E* **84**, 046117 (2011).
 - [9] T. Squartini, G. Fagiolo, and D. Garlaschelli, *Phys. Rev. E* **84**, 046118 (2011).
 - [10] M. Di Vece, D. Garlaschelli, and T. Squartini, *Phys. Rev. Research* **4**, 033105 (2022).
 - [11] J. M. Swaminathan, S. F. Smith, and N. M. Sadeh, *Decision sciences* **29**, 607 (1998).
 - [12] R. De Souza, S. Zice, and L. Chaoyang, *Integrated Manufacturing Systems* (2000).
 - [13] T. Y. Choi, K. J. Dooley, and M. Rungtusanatham, *Journal of Manufacturing Systems* **23**, 529 (2004).

- nal of Operations Management **19**, 351 (2001), ISSN 1873-1317.
- [14] D. Ivanov, B. Sokolov, and A. Dolgui, International Journal of Production Research **52**, 2154 (2014), ISSN 0020-7543.
- [15] A. Świerczek, International Journal of Production Economics **157**, 89 (2014), ISSN 0925-5273.
- [16] B. B. M. Shao, Z. M. Shi, T. Y. Choi, and S. Chae, Decision Support Systems **114**, 37 (2018), ISSN 0167-9236.
- [17] C. Diem, A. Borsos, T. Reisch, J. Kertész, and S. Thurner, Sci Rep **12**, 7719 (2022), ISSN 2045-2322.
- [18] B. Carreras, V. Lynch, M. Sachtjen, I. Dobson, and D. Newman, in *Proceedings of the 34th Annual Hawaii International Conference on System Sciences* (2001), pp. 719–727.
- [19] C. D. Brummitt, R. M. D’Souza, and E. A. Leicht, Proceedings of the National Academy of Sciences **109**, E680 (2012).
- [20] R. Carvalho, L. Buzna, F. Bono, E. Gutiérrez, W. Just, and D. Arrowsmith, Phys. Rev. E **80**, 016106 (2009).
- [21] A. Maritan, A. Rinaldo, R. Rigon, A. Giacometti, and I. Rodríguez-Iturbe, Phys. Rev. E **53**, 1510 (1996).
- [22] P. S. Dodds and D. H. Rothman, Phys. Rev. E **63**, 016115 (2000).
- [23] P. S. Dodds and D. H. Rothman, Phys. Rev. E **63**, 016116 (2000).
- [24] A. Rinaldo, J. R. Banavar, and A. Maritan, Water Resources Research **42** (2006), ISSN 1944-7973.
- [25] G. B. West, J. H. Brown, and B. J. Enquist, Science **276**, 122 (1997).
- [26] J. R. Banavar, A. Maritan, and A. Rinaldo, Nature **399**, 130 (1999), ISSN 1476-4687.
- [27] B. J. Enquist, J. H. Brown, and G. B. West, Nature **395**, 163 (1998), ISSN 1476-4687.
- [28] J. D. Damuth, Nature **395**, 115 (1998), ISSN 1476-4687.
- [29] G. B. West, J. H. Brown, and B. J. Enquist, Nature **400**, 664 (1999), ISSN 1476-4687.
- [30] M. E. J. Newman, S. H. Strogatz, and D. J. Watts, Phys. Rev. E **64**, 026118 (2001).
- [31] S. M. Shekatkar, figshare (2022), URL https://figshare.com/articles/software/dependency-networks_python_package_/13275137.